A Prism-Based Optical Readout Method for MEMS Bimaterial Infrared Sensors

Ulas Adiyan, *Student Member, IEEE*, Fehmi Civitci, Onur Ferhanoglu, Hamdi Torun, *Member, IEEE*, and Hakan Urey, *Senior Member, IEEE*

***Abstract*— This letter demonstrates a novel prism-based optical-readout, which uses a single prism to detect the incoming TM polarized wave just below the critical angle. The method is used with a 35-μm-pixel pitch MEMS thermal sensor, whose inclination angle changes with the absorbed infrared (IR) radiation that results in an increase in the reflectivity at the prism's glass–air interface. We compared this approach with the conventional knife-edge method. Noise equivalent temperature difference for a single sensor was measured as 200 mK for knife-edge method, and 154 mK for the proposed critical angle approach. Our approach shows a significant improvement for the sensitivity of the IR sensor. Both methods utilize an AC-coupled readout method for a single MEMS pixel using a photodetector, which responds only to changes in the scene. This method can be scaled to achieve smart pixel cameras for read sensor arrays with low-noise and high-dynamic range.**

***Index Terms*— Thermo-mechanical MEMS, IR detection, optical readout, AC coupling, critical angle.**

I. Introduction

UNCOOLED bimaterial sensors convert absorbed IR radiation to mechanical motion owing to the mismatch in the thermal expansion coefficients of the bimaterial legs. For a one-end fixed cantilever-type device (Fig.1), this motion induces a small tilt and can be detected via optical methods. Commonly used optical readout methods for bimaterial sensors are optical lever readout [1]–[3], knife edge filtering [4], [5] and optical interferometry [6], [7]. Generally, the performance of these methods is limited by the reduced dynamic range due to a DC bias on the photodetectors or CCDs of the detection system. Prior work demonstrated a performance improvement for a 35-μm pitch single MEMS sensor element using an AC-coupled technique [8], showcasing Noise Equivalent Temperature Difference (NETD) of 216 mK for diffraction grating-based readout [8], and 198 mK for knife-edge method (KEM) [9]. The AC-coupled optical readout is implemented by the elimination of the DC bias, which mitigates the DC related noise term and improves the sensitivity of the sensor.

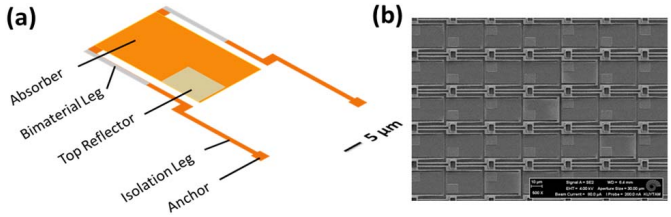

Fig. 1. (a) The geometry of single sensor element. (b) Scanning Electron Microscope (SEM) Image of a part of the array.

Fig.1a shows the designed and fabricated MEMS sensor geometry, which is suitable for optical lever based readout. The pixel is 35 μm in pitch size and made of 150 nm-thick aluminum and 150 nm-thick silicon nitride forming the bimaterial layer. The lengths and thicknesses of the legs are optimized considering thermal isolation, and induced displacements due to the temperature change in the sensor. The 40 μm-long isolation legs provide 1.2×10^{-7} W/K thermal conductivity, resulting in a thermal time constant of 1.5 ms that is suitable for real-time imaging. The 20 μm-long bimaterial legs provide $>$ 40 nm/°C responsivity (Fig.2).

The fabrication process of the cantilevers follows the recipe described previously [8]. This design does not require diffraction gratings, which simplifies the fabrication steps, improving effective absorption area since the area of the top reflector can be reduced, and eliminates the need for pixel surface planarization to avoid the tilt errors. Fig.1b shows a SEM image of a portion of the MEMS focal plane array.

We use Finite Element Method (FEM) to design the sensor structure. IR induced temperature change on the sensor creates a thermal gradient along the pixel, as illustrated in Fig.2a that induces a tilt over the sensor with respect to its substrate (Fig.2b). The thermo-mechanical responsivity was also verified with heating experiments under a white light interferometer (WLI) device. We directly heated up our MEMS device using a thermo-electric cooler (TEC). Measurements under WLI revealed a tilt angle vs. temperature change of 0.08°/1°C as opposed to the simulation result of 0.11°/1°C (corresponding to thermo-mechanical displacement gradient over the MEMS reflector), extracted from FEM (Fig.2c). We attribute the deviation between the measured values and the simulated ones to the deviation of the geometry and material properties from the theoretical values.

With an aim of further improving the response of the sensor, here we developed an optical readout method using a glass prism so that the tilt angle of the sensor results in a change in the reflectivity of a glass-air interface, utilizing the

Manuscript received February 17, 2016; revised May 3, 2016; accepted May 24, 2016. Date of publication May 30, 2016; date of current version June 30, 2016. This work was supported by the Scientific and Technological Research Council of Turkey (TÜBITAK) under Grant 114E882.

U. Adiyan and H. Urey are with the Electrical and Electronics Engineering Department, Koç University, Istanbul 34450, Turkey (e-mail: uladiyan@ku.edu.tr; hurey@ku.edu.tr).

F. Civitci and O. Ferhanoglu are with the Electronics and Communication Engineering Department, Istanbul Technical University, Istanbul 34469, Turkey (e-mail: civitci@itu.edu.tr; ferhanoglu@itu.edu.tr).

H. Torun is with the Electrical and Electronics Engineering Department, Boğaziçi University, Istanbul 34342, Turkey (e-mail: hamdi.torun@boun.edu.tr).

Color versions of one or more of the figures in this letter are available online at http://ieeexplore.ieee.org.

Digital Object Identifier 10.1109/LPT.2016.2574123

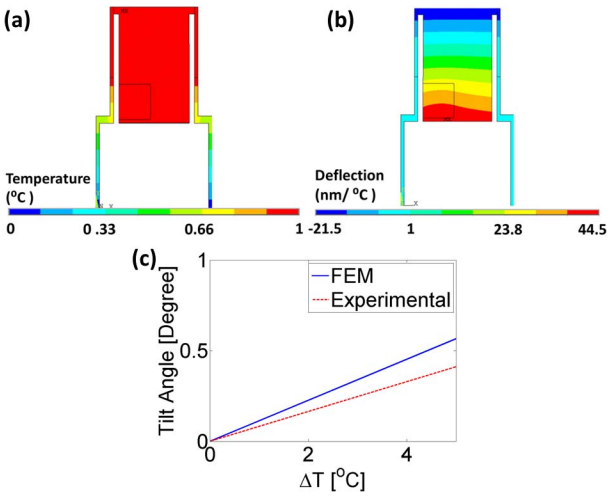

Fig. 2. FEM Analysis: (a) Thermal Gradient of the single sensor element due 1 °C input on the absorber where anchors are fixed at 0 °C. (b) Mechanical deflection analysis for the thermal gradient in (a). (c) Comparison of the tilt angles w.r.t. temperature using the experimental data and the FEM results.

critical-angle phenomena. Various prism based methods have been utilized before for angle sensing: (i) Reflection near the critical angle was used for highly sensitive position measurement for a single bulky mirror mounted on a rotational stage [10], (ii) A similar method, which uses non-polarized light in the optical readout, is also used as a readout method for bimaterial IR sensor arrays in order to implement optical background subtraction, however, at the expense of lower responsivity as opposed to polarized light and unilateral readout capability (works only for heating or cooling case) [11]. Here, we used a TM polarized wave, which has higher responsivity on the reflectivity curve with respect to the incident angle of the incoming wave, as compared to a TE polarized or non-polarized wave near the critical angle. We further implement AC coupled optical detection for background subtraction. Although the performance of this method is demonstrated by using a single pixel in this letter, prism-based optical readout is also suitable for array imaging.

In Section II, we described the method of AC-coupled detection with the critical angle method (CAM). Section III presents the simulation results and comparison of both methods and Section IV presents the experimental results.

II. AC Coupled Optical Readout Using Critical Angle Approach

Fig.3a illustrates the AC coupled optical readout setup for the KEM, utilizing tilting pixel structures and filtering at the knife-edge filter plane [9]. The laser light is focused onto a single sensor, placed in a vacuum chamber ($\sim$ 1mTorr), and the reflected light is captured on a PD with a 4f optical system. The CCD camera is used for checking the alignment of the laser beam to the selected MEMS sensor for the single MEMS pixel operation as described in [9] for both methods. The knife-edge filter modulates the optical power and changes the intensity at the image plane with the sensor's tilt motion.

Fig.3b shows the proposed optical readout setup, which utilizes a critical angle approach for a TM polarized wave. The illumination optics for the prism-based readout is nearly identical to the conventional method, with the exception of

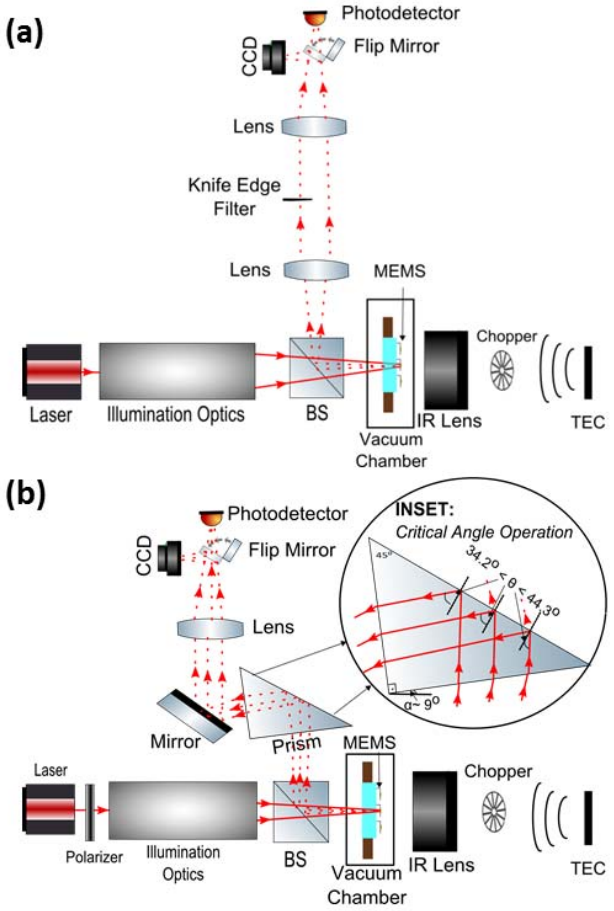

Fig. 3. Experimental setup for the characterization of single sensor element using different AC coupled optical readout methods: (a) Knife-edge method, KEM. (b) Critical angle method, CAM. The CCD was used to check the alignment of laser with the selected sensor for single MEMS pixel operation.

an additional polarizer for polarization control. After being polarized and directed to the MEMS sensor, the laser beam reflects back to the beam splitter.

The key element of the proposed optical system is the glass prism. One has to provide an initial tilt to the prism in order to obtain an operation with high responsivity as shown in the inset of Fig.3b. Since we focus the light onto the reflector of the MEMS pixel, the rays will reflect with different angles whose spread is based on the numerical aperture (NA) of the focusing lens and the size of the MEMS reflector. In this case, the reflector plane of the prism's glass-air interface forms a virtual reflection matrix, which has different reflection coefficients corresponding to different ray angles. The change in the inclination angle of the MEMS sensor results in a change in the experienced reflection values. Therefore, there is no need for a Fourier lens or spectral filtering for light modulation. Laser light that is reflected off the prism is collected via a lens at the PD.

Finally, for both setups the intensity data, in response to the chopped IR target, is collected at the PD, which is connected to a wide band-pass filter a bandwidth of 88.5 Hz with the low and high 3 dB cutoff frequencies $f_{LOW} = 1.5$ Hz, $f_{HIGH} = 90$ Hz providing the AC-coupled sensing. The AC-coupled operation that is applied to both methods (CAM, KEM) is convenient for single sensor operations. Furthermore, it is feasible to scale up this method for a large

array using a customized CMOS ROIC (readout integrated circuit) [12].

III. Simulation Results

A simple model based on beam propagation is developed in MATLAB in order to compare the sensitivities of both methods. The numerical simulations of optical beam propagations are carried out by angular spectrum method [13].

In our model, change in the target temperature from 25 °C to 525 °C is first converted to the temperature change on the detector (based on 302:1 ratio between target and detector temperature that is determined by the thermal conductivity of the sensor, emissivity of the target, and IR transmittance of the system [7]), which is then converted to the corresponding sensor tilt based on FEM findings (Fig.2b). This corresponds to an angular displacement of 0.38° at the prism's entrance plane which is then converted to 0.25° after refraction.

For the KEM propagation simulations, the red laser beam (λ = 633 nm) having 12 mm diameter after magnification, is first focused on the MEMS pixel via a lens (f=100mm). The light reflected from the square MEMS reflector is then back-propagated. The beam is collimated with another lens (f=100 mm) after propagating a 100 mm distance from the pixel and reaching its initial size. The beam is then knife-edge filtered, blocking half of the beam [4], [5], at room temperature. Fig.4a shows the spatially filtered beams demonstrating KEM simulation just after the knife-edge filter. The change of detector temperature causes the MEMS sensor to tilt, which shifts the beam position at the knife-edge plane, resulting in a change of detected optical intensity.

In the CAM, the mechanical tilt motion due to the detector temperature change is directly converted to a change in the incident angle on the prism's glass-air interface, which affects the reflection experienced by the beam. The simulation includes the effects of different angles coming from the MEMS reflector, based on the NA of the focusing lens and the size of the MEMS reflector. These different angles correspond to a reflection matrix with different reflection coefficients that is formed on the prism's glass-air interface for a TM polarized wave. The change of the beam position with respect to the reflection matrix leads to an increase for the intensity of the light at the PD plane (Fig.4b), owing to the significantly increased reflection coefficients. The secondary lobe of the beam profile in the horizontal direction is significantly enhanced due experiencing a high reflection coefficient. Fig.4c illustrates the reflectivity of a glass (n_glass = 1, 51)-air (n_air = 1) interface with respect to the angle of incidence. The inset shows the change of the reflectivity around $39° < \theta < 41°$, where the brighter parts of the beam is exposed to a reflection change with a high responsivity. In our model, the initial tilt angle of the prism is optimized as $\alpha = 9°$, resulting in maximum responsivity. The reflection angles vary in the range of $34.2° < \theta < 44.3°$ at the prism's glass-air interface for our simulation window that is limited by the aperture size of the prism. The simulation takes the angle spread into account, which forms the 2D reflection matrix at the prism's glass-air interface, as illustrated in Fig.4d.

Fig.4e compares the change of normalized intensity for both KEM and CAM. Background subtraction is applied to the beams at the room temperature for both methods to focus on the changes in the scene. Therefore, the normalization took

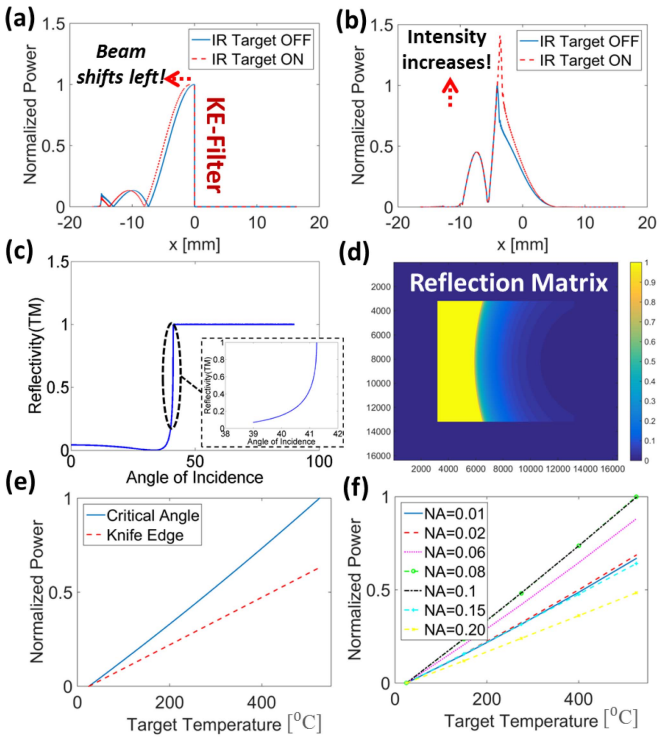

Fig. 4. Beam propagation simulation results (Sample intervals in space domain are dx = dy = 2 um.) showing the cross-sections (y = 0) of the beams according to the two different target temperatures (25 °C and 525 °C) for (a) Knife-edge method, KEM. (b) Critical angle method, CAM. (c) Reflectivity of a glass (n = 1, 51) – air interface (n = 1) for TM polarization. (d) Reflection matrix at the prism (glass-air) interface. (e) Comparison of normalized power changes for both approaches at PD w.r.t. different target temperatures. (f) Results for the normalized power changes at PD w.r.t. different target temperatures using CAM for different illumination angles.

place through linear mapping of the power increase obtained for the CAM to values between 0 (25 °C room temperature) and 1 (525 °C target). Since the angle change at the prism's reflector plane is very small ($\Delta\theta = 0.25°$) even for a 525 °C target, the change in the reflectivity and in the power of the optical signal is considerably linear with a maximum deviation of 3% from the linear fit. Assuming an NETD of 150 mK, our method's dynamic range will be 3500 which corresponds to nearly 12 bits. Furthermore, the change in the signal power for a 50 °C target is perfectly linear due to an even smaller angle change. The same linear transformation is applied on the KEM results, revealing a normalized intensity change of 0.63. We conclude that the critical angle approach provides a higher sensitivity than the conventional KEM.

Lastly we analyzed the effect of the angular spread of the beam on the responsivity of the optical readout. The NA of the illumination optics is 0.06 for the previous simulations, which exhibits one of the higher responsivities (Fig.4f). For the smaller NA case (NA=0.01-0.02), the diffraction spread related to the MEMS reflector size will be dominant. For the larger NA case (NA=0.15-0.20), the angular spread depends on the NA itself. As a result, NA can be optimized for a better responsivity by considering the size of the MEMS reflector.

IV. Experimental Results

A black painted TEC was used as a blackbody target and it was calibrated with an IR thermometer (EXTECH / IR201A).

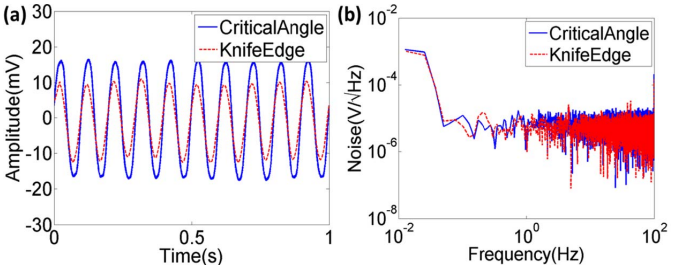

Fig. 5. (a) AC coupled photodetector signal obtained using a chopper blade (at 25°C) rotating at 10 Hz placed in front of an IR target (at 50°C) for knife-edge method (KEM) and Critical angle method (CAM). (b) Noise levels of the optical readout system for both methods.

TABLE I
NETD VALUES FOR DIFFERENT OPTICAL READOUT METHODS

Optical Readout Method	NETD [mK]
Critical Angle	154
Knife-Edge	200

At room temperature, we equalized the DC light levels at the PD for both methods by placing neutral density (ND) filters within the "illumination optics" part of the optical setup. The radiation of the 50 °C target was chopped at 10 Hz. The responses of the selected sensor for both KEM and CAM are shown in Fig.5a. The location of the knife-edge filter for KEM and the tilt angle of the prism for the CAM were optimized to obtain the maximum signal levels. The peak-to-peak signal level was observed to be 33 mV for the CAM and 22 mV for the KEM, exhibiting a 50% increase in the signal level. The amount of improvement in the signal output, perfectly matches our findings based on beam propagation simulations.

Fig.5b shows the noise levels for both methods at room temperature, which exhibit similar characteristics due to the mentioned equalization of the DC light levels at the PD. We integrated the noise between 0–30 Hz for extracting SNR and NETD of the system. The noise spectrum was limited to 0–30 Hz as an ideal case to characterize the system, as capturing 15 Hz video content with Nyquist rate, for real time video applications. The detailed noise analysis with SNR and NETD calculations can be found in [8].

NETD values were calculated according to a target with a temperature difference of Δ T = 25 °C. The NETD values of the selected sensor for both methods are given in Table I. The experimentally determined NETD values are 154 mK for CAM and 200 mK for KEM using an f/0.86 IR lens. Critical angle approach decreased the NETD of the IR sensor 25%, revealing a significant improvement in the system sensitivity for the indicated target temperatures. The improved NETD value of 154 mK is comparable to the state-of-the-art bimaterial IR sensors that are larger in size [1]–[5], owing to the prism-based and AC-coupled readout.

V. CONCLUSION

A novel optical readout method using a single prism is developed, employing detection at the glass-air interface of the prism for a TM wave near the critical angle. We compared this approach with the conventional KEM for an IR sensor. Both methods employ AC-coupled sensing that responds only to the changes in the scene to eliminate DC bias signal, and thus DC noise component, at the PD. NETD for a single sensor was measured as 200 mK using the KEM, and 154 mK for the CAM, revealing a 25% improvement of sensor sensitivity accompanied by %50 improvement in the signal amplitude. The difference between the improvements in the sensor sensitivity vs. the signal amplitude is caused by slightly different noise levels, possibly due to random vibrations that are induced in the setup. The proposed CAM offers high sensitivity through precise tuning of the initial angle of incidence by rotating the prism. Our approach is adaptable to array imaging through collimated illumination. For the array operation, the diffraction spread will solely be determined by the aperture (MEMS reflector) size, which will in turn set the initial prism angle for optimal responsivity. Non-uniformity in the arrays may be a problem for both CAM and KEM as each pixel will have different initial angles and sensitivity levels. Non-uniformity can be fixed through the use of look-up tables or a shutter temperature calibration routine.

The readout method has been demonstrated for IR sensing applications. The method is also applicable to other types of sensors, where optical displacement readout is implemented.

REFERENCES

[1] L. R. Senesac, J. L. Corbeil, S. Rajic, N. V. Lavrik, and P. G. Datskos, "IR imaging using uncooled microcantilever detectors," *Ultramicroscopy*, vol. 97, nos. 1–4, pp. 451–458, Oct./Nov. 2003.
[2] D. Grbovic *et al.*, "Uncooled infrared imaging using bimaterial micro-cantilever arrays," *Appl. Phys. Lett.*, vol. 89, no. 7, p. 073118, 2006.
[3] M. Erdtmann, L. Zhang, G. Jin, S. Radhakrishnan, G. Simelgor, and J. Salerno, "Optical readout photomechanical imager: From design to implementation," *Proc. SPIE*, vol. 7298, pp. 72980I-1–72980I-8, May 2009.
[4] B. Jiao *et al.*, "An optical readout method based uncooled infrared imaging system," *Int. J. Infr. Millim. Waves*, vol. 29, no. 3, pp. 261–271, 2008.
[5] F. Dong *et al.*, "An uncooled optically readable infrared imaging detector," *Sens. Actuators A, Phys.*, vol. 133, no. 1, pp. 236–242, 2007.
[6] U. Adiyan, F. Çivitçi, R. B. Erarslan, O. Ferhanoğlu, H. Torun, and H. Urey, "Simultaneous two-wavelength readout for thermo-mechanical MEMS detectors," in *Proc. Int. Conf. Opt. MEMS Nanophoton. (OMN)*, Glasgow, Scotland, Aug. 2014, pp. 169–170.
[7] M. F. Toy, O. Ferhanoğlu, H. Torun, and H. Urey, "Uncooled infrared thermo-mechanical detector array: Design, fabrication and testing," *Sens. Actuators A, Phys.*, vol. 156, no. 1, pp. 88–94, Nov. 2009.
[8] U. Adiyan, F. Çivitçi, O. Ferhanoğlu, H. Torun, and H. Urey, "A 35-μm pitch IR thermo-mechanical MEMS sensor with AC-coupled optical readout," *IEEE J. Sel. Topics Quantum Electron.*, vol. 21, no. 4, Jul./Aug. 2015, Art. no. 2701306.
[9] U. Adiyan, F. Çivitçi, O. Ferhanoğlu, H. Torun, and H. Urey, "MEMS bimaterial IR sensor array with AC-coupled optical readout," in *Proc. Int. Conf. Opt. MEMS Nanophoton. (OMN)*, Jerusalem, Israel, Aug. 2015, pp. 1–2.
[10] J. Villatoro and A. García-Valenzuela, "Measuring optical power transmission near the critical angle for sensing beam deflection," *Appl. Opt.*, vol. 37, no. 28, pp. 6648–6653, 1998.
[11] C. Gong, Y. Zhao, L. Dong, X. Yu, P. Chen, and W. Liu, "All-optical background subtraction readout method for bimaterial cantilever array sensing," *Opt. Exp.*, vol. 23, no. 16, pp. 20576–20581, 2015.
[12] R. B. Erarslan *et al.*, "Design and characterization of micromachined sensor array integrated with CMOS based optical readout," *Sens. Actuators A, Phys.*, vol. 215, pp. 44–50, Aug. 2014.
[13] J. W. Goodman, *Introduction to Fourier Optics*, 3rd ed. New York, NY, USA: McGraw-Hill, 2005, ch. 3.10, pp. 55–61.